

## MINI REVIEW

[View Article Online](#)  
[View Journal](#) | [View Issue](#)



Cite this: *Ind. Chem. Mater.*, 2023, 1, 93

## Multicomponent catalyst design for $\text{CO}_2/\text{N}_2/\text{NO}_x$ electroreduction

Shunhan Jia, <sup>ab</sup> Limin Wu, <sup>ab</sup> Liang Xu, <sup>a</sup> Xiaofu Sun, <sup>ab</sup> and Buxing Han <sup>abc</sup>

Electroreduction of small molecules such as  $\text{CO}_2$ ,  $\text{N}_2$ , and  $\text{NO}_3^-$  is one of the promising routes to produce sustainable chemicals and fuels and store renewable energy, which could contribute to our carbon neutrality goal. Emerging multicomponent electrocatalysts, integrating the advantages of individual components of catalysts, are of great importance to achieve efficient electroreduction of small molecules via activation of inert bonds and multistep transformation. In this review, some basic issues in the electroreduction of small molecules including  $\text{CO}_2$ ,  $\text{N}_2$ , and  $\text{NO}_3^-$  are briefly introduced. We then discuss our fundamental understanding of the rule of interaction in multicomponent electrocatalysts, and summarize three models for multicomponent catalysts, including type I, “a non-catalytically active component can activate or protect another catalytic component”; type II, “all catalytic components provide active intermediates for electrochemical conversion”; and type III, “one component provides the substrate for the other through conversion or adsorption”. Additionally, an outlook was considered to highlight the future directions of multicomponent electrocatalysts toward industrial applications.

Received 8th December 2022,  
Accepted 28th December 2022

DOI: 10.1039/d2im00056c

rsc.li/icm

Keywords: Green chemistry; Green carbon science; Electrocatalysis; Synergetic effect.

## 1 Introduction

The chemical industry plays a crucial role in the historical evolution of society, but it causes emerging environmental concerns and skyrocketing  $\text{CO}_2$  emissions.<sup>1–3</sup> Recently, green chemistry and chemical engineering have opened sustainability possibilities through transforming renewable feedstocks, such as  $\text{CO}_2$  and  $\text{NO}_x$  ( $\text{N}_2$  and  $\text{NO}_3^-$ ), into environmentally friendly chemicals, including syngas, hydrocarbons, oxygenates and ammonia. However, the existence of inert bonds, *e.g.*, the  $\text{C}=\text{O}$  bond in  $\text{CO}_2$  and the  $\text{N}\equiv\text{N}$  bond in  $\text{N}_2$ , brings both restricted thermodynamics and sluggish kinetics to the activation and conversion of these molecules to synthesize sustainable chemicals.<sup>4–6</sup> Among the developed strategies, the electrochemical conversion method provides a universal carbon-neutral route to efficiently upgrade green chemical sources with inert bonds to chemicals and fuels under ambient conditions

harnessing clean energy.<sup>7</sup> Previous studies proved that  $\text{CO}_2$  could be electrochemically converted to value-added chemicals and fuels, such as formic acid,  $\text{CO}$ , methanol, ethene and ethanol.<sup>8–10</sup> Recently, electrochemical synthesis of ammonia from  $\text{N}_2$  and  $\text{NO}_3^-$  has been also developed, giving new life to  $\text{NH}_3$  synthesis.

The active components of catalysts are the essential building blocks of the modern chemical research and chemical industry.



Shunhan Jia

<sup>a</sup> Beijing National Laboratory for Molecular Sciences, CAS Key Laboratory of Colloid and Interface and Thermodynamics, CAS Research/Education Center for Excellence in Molecular Sciences, Institute of Chemistry, Chinese Academy of Sciences, Beijing, 100190, China. E-mail: sunxiaofu@iccas.ac.cn, hanbx@iccas.ac.cn

<sup>b</sup> School of Chemical Sciences, University of Chinese Academy of Sciences, Beijing, 100049, China

<sup>c</sup> Shanghai Key Laboratory of Green Chemistry and Chemical Processes, School of Chemistry and Molecular Engineering, East China Normal University, Shanghai, 200062, China

Shunhan Jia received his B.S. degree in Chemistry from Nankai University working with Prof. Zhiqiang Niu on the design and fabrication of flexible aqueous zinc-ion batteries. After his undergraduate research stay in Prof. Enzheng Shi's group at Westlake University focusing on 2D halide perovskite heterostructures, he started to pursue his Ph.D. under the supervision of Prof. Buxing Han and Prof. Xiaofu Sun at the Institute of Chemistry, Chinese Academy of Sciences (CAS). His research interests now center on multicomponent catalysts and the transformation of inert molecules (*e.g.*,  $\text{CO}_2$  and  $\text{N}_2$ ) into value-added chemicals using renewable energy.

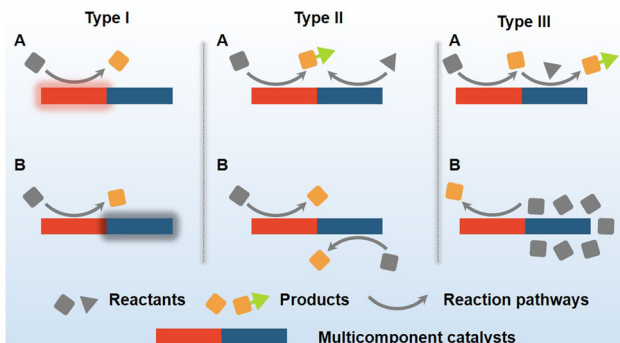


In a typical electrocatalytic process, active components could serve as intermediates between carriers and the adsorbed intermediates to promote the redox half-reaction.<sup>11</sup> Monocomponent electrocatalysts face the disadvantages of poor stability, limited activity, and restricted reaction processes. Thus, the multicomponent design of electrocatalysts has attracted widespread attention.<sup>12</sup> In this review, we first briefly introduced basic issues in the electroreduction of small molecules including  $\text{CO}_2$ ,  $\text{N}_2$ , and  $\text{NO}_3^-$ , which will be taken as typical examples for further discussion. We then systematically shared our fundamental understanding of three models for multicomponent catalysts as is shown in Scheme 1.

Type I: a non-catalytic active component can activate or protect another catalytic component.

Type II: all catalytic components provide active intermediates for electrochemical conversion.

Type III: one component provides the substrate for the other through conversion or adsorption.



Scheme 1 Models of multicomponent electrocatalysts.

Further, centering around the electroreduction of small molecules, we presented recent developments in multicomponent catalysts using the listed models. Future directions were finally discussed for applying



Limin Wu

Limin Wu received her B.E. degree in Materials Science and Engineering from Hebei University of Technology. She started to pursue her Ph.D. under the supervision of Prof. Xiaofu Sun at the Institute of Chemistry, Chinese Academy of Sciences (CAS). Her research is focused on the utilization and conversion of nitrate.



Liang Xu

Liang Xu received her Ph.D. degree in Chemical Engineering and Technology from Beijing University of Chemical Technology in 2019. Currently, she is working as a post-doctoral fellow with Prof. Buxing Han and Prof. Xiaofu Sun at the Institute of Chemistry, Chinese Academy of Sciences (CAS). Her research interests mainly focus on the electrocatalytic conversion of  $\text{CO}_2/\text{NO}_x$  into high value-added chemicals.



Xiaofu Sun

Xiaofu Sun received his B.S. degree in Chemistry from Nankai University in 2011 and M.S. degree in Physical Chemistry from Renmin University of China in 2014. He earned his Ph.D. degree at the Institute of Chemistry, Chinese Academy of Sciences (CAS) in 2017, and did postdoctoral research at Nanyang Technological University. He has been a professor at the Institute of Chemistry, CAS, since 2019. His current research interests

cover utilization and conversion of  $\text{CO}_2/\text{NO}_x$  applications of green solvents (e.g.,  $\text{H}_2\text{O}$ , ionic liquids), and design and synthesis of novel catalysts and catalytic systems.



Buxing Han

Buxing Han received his Ph.D. degree from the Institute of Chemistry, Chinese Academy of Sciences (CAS) in 1988, and did postdoctoral research from 1989 to 1991 at the University of Saskatchewan, Canada. He has been a professor at the Institute of Chemistry, CAS, since 1993. He is an Academician of CAS and a Fellow of the Royal Society of Chemistry, a titular member of the Organic and Biomolecular Chemistry Division, IUPAC, and

was the Chairman of the IUPAC Subcommittee on Green Chemistry from 2008 to 2012. He works in the interdisciplinary area of Physical Chemistry and Green Chemistry. His research interests include properties of green solvent systems and applications of green solvents in chemical reactions and materials science.



multicomponent electrocatalysts in the industrial utilization of renewable chemical sources through highly efficient activation and conversion of inert bonds.

## 2 Electrochemical reduction of CO<sub>2</sub>/N<sub>2</sub>/NO<sub>x</sub>

### 2.1 Electroreduction of CO<sub>2</sub> to chemicals and fuels

CO<sub>2</sub> is the main greenhouse gas but is also demonstrated as a promising C<sub>1</sub> chemical source. Due to its controlled pathways, simple reaction unit, green process, and scale-up potential, the electrochemical CO<sub>2</sub> reduction reaction (CO<sub>2</sub>-RR) is a promising way to convert CO<sub>2</sub> to value-added chemicals and fuels with H<sub>2</sub>O as the proton source and store increasingly produced clean electricity.<sup>13</sup> Researchers have succeeded to obtain CO, methanol (CH<sub>3</sub>OH), formic acid (HCOOH), methane (CH<sub>4</sub>), ethanol (CH<sub>3</sub>CH<sub>2</sub>OH), ethene (C<sub>2</sub>H<sub>4</sub>), and other chemicals from the CO<sub>2</sub>-RR.<sup>13–15</sup> The carbon energy index (CEI, Fig. 1A) is newly defined in green carbon science to describe carbon-containing molecules with their atomic ratio (C/C, H/C, and O/C).<sup>2</sup> Understandably, molecules with larger N<sub>H</sub>/N<sub>C</sub> are favorable to release energy. A semiquantitative overview of common CO<sub>2</sub>-RR products is presented in Fig. 1B with data from ref. 16 and 17. The techno-economic analysis of the CO<sub>2</sub>-RR over various catalysts, electrolytes, and cells with accurate data has been well discussed in several literature reports, which will not be discussed in detail in the current minireview.<sup>16–20</sup> Briefly, obvious disadvantages exist in HCOOH compared to other products. Despite the high CEI of CH<sub>4</sub>, high electricity cost hinders the further application of CO<sub>2</sub>-to-CH<sub>4</sub>. Conversely, CO, CH<sub>3</sub>OH, and C<sub>2</sub> chemicals from the CO<sub>2</sub>-RR are

economically feasible, technologically accessible, and of great potential in the carbon-neutral future.

As is shown in Fig. 2A, the electroreduction of CO<sub>2</sub> with H<sub>2</sub>O to various target molecules is a complex proton-coupled electron transfer process.<sup>15</sup> Generally, the CO<sub>2</sub> molecule could first transform into CO<sub>2</sub><sup>–</sup> and \*CO after being adsorbed into the electrode guided by different catalysts. The CO<sub>2</sub><sup>–</sup> and \*CO intermediates could directly desorb from the electrode for the formation of C<sub>1</sub> products such as HCOOH and CO. However, to produce more useful products discussed in Fig. 2A, multi-step electroreduction with active H species, C–C coupling, and multi-step transformation are necessary, in which multicomponent catalysts summarized here are thus needed.

### 2.2 Electroreduction of N<sub>2</sub> and NO<sub>3</sub><sup>–</sup> to NH<sub>3</sub>

The industrial Haber–Bosch process is of great importance to modern society since it could produce useful NH<sub>3</sub> from N<sub>2</sub> and H<sub>2</sub>. Nonetheless, highly energy-intensive, huge CO<sub>2</sub> emissions from the generation of H<sub>2</sub> and centralized facilities are the main drawbacks of the current Haber–Bosch process making it unsustainable. Electrochemical reduction of N<sub>2</sub> and its derivatives such as NO<sub>3</sub><sup>–</sup> with H<sub>2</sub>O as the proton source provides a sustainable and carbon-neutral way to synthesize NH<sub>3</sub>.<sup>6</sup> Nonetheless, activation and conversion of the inert bonds in N<sub>2</sub> and NO<sub>3</sub><sup>–</sup> are inherently challenging because of their thermodynamic stability.<sup>21</sup> The electrochemical N<sub>2</sub> reduction reaction (NRR) in Fig. 2B is usually based on dissociative and associative mechanisms.<sup>22</sup> In the dissociative mechanism, N<sub>2</sub> molecules adsorbed on the electrode surface could undergo the activation of the N–N bond first with high energy input. Meanwhile in the associative mechanism, two nitrogen atoms could link with each other until the formation of one NH<sub>3</sub> molecule. In addition, these two pathways could occur alternately through the in-turn hydrogenation of two nitrogen atoms to form two NH<sub>3</sub> molecules. As for the nitrate reduction reaction (NITRR) shown in Fig. 2C, the conversion of NO<sub>3</sub><sup>–</sup> to \*NO<sub>2</sub><sup>–</sup> is the first step, followed by the reduction of \*NO<sub>2</sub><sup>–</sup> to \*NO, which could undergo multistep transformation to NH<sub>3</sub> with \*NH<sub>2</sub>OH as the key intermediate.<sup>23,24</sup> Hence, both the NRR and NITRR are also complex and require multicomponent electrocatalysts to drive the reactions with enhanced efficiency. In addition, electroreduction of other NO<sub>x</sub> molecules, such as NO (x = 1) and NO<sub>2</sub><sup>–</sup> (x = 2), to NH<sub>3</sub> has been also reported but will not be discussed in the current review.<sup>25–28</sup>

## 3 Emerging multicomponent catalysts

### 3.1 Type I multicomponent catalysts

#### 3.1.1 Models of multicomponent catalysts.

Multicomponent catalysts, as the name implies, have at least two components, but it is worth noting that not all the components in a multicomponent catalyst act as catalytic sites for catalytic reactions. The main characteristic of a type I

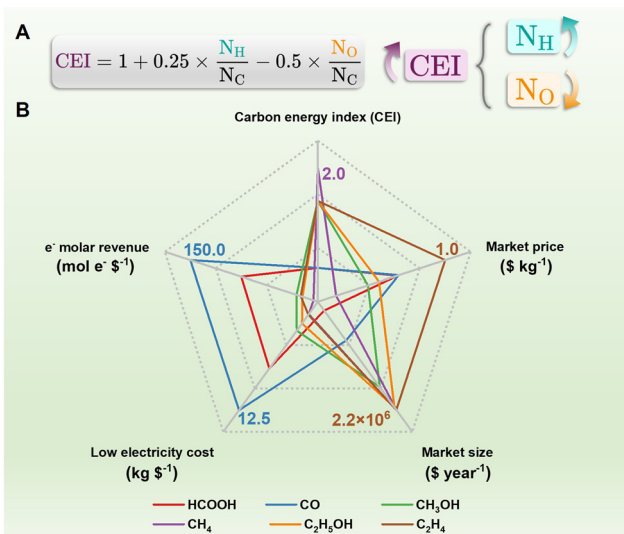


Fig. 1 (A) The formula to calculate the carbon energy index (CEI) of different carbon-containing molecules. N<sub>X</sub> (X = C, H, and O): the number of X atoms in the molecule. (B) An overview of common CO<sub>2</sub>-RR products from the perspective of both chemistry and economics.



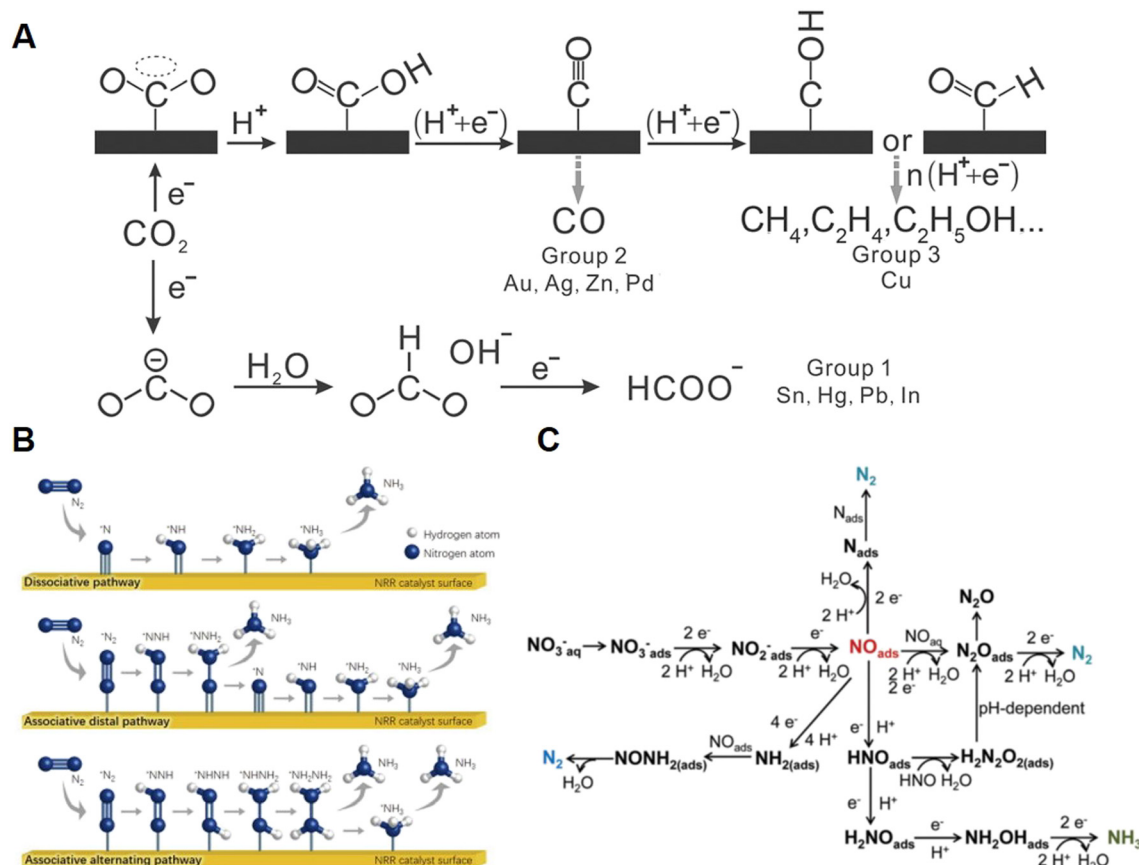


Fig. 2 (A) The possible pathways of multi-step activation and transformation of  $\text{CO}_2$  to various value-added products. Reprinted with permission from ref. 15. Copyright 2016, John Wiley & Sons, Inc.; Proposed roadmap of multi-step electroreduction of (B)  $\text{N}_2$  and (C)  $\text{NO}_3^-$  towards  $\text{NH}_3$  synthesis. Reprinted with permission from ref. 22 and 23. Copyright 2019, Elsevier and Copyright 2021, the Royal Society of Chemistry.

(Scheme 1) multicomponent catalyst is that only one component acts as the active center during the catalytic reaction. The other component could enhance the activity and stability of the catalytic reaction by activating the main component or preventing its degradation. For instance, as is shown in type I-A, in a multicomponent catalyst, A/B, A is the true active site, while B has only low or virtually no catalytic activity. In the catalytic reaction, A could be activated by B to  $\text{A}^+$ , so it has high activity. For instance, researchers discovered that B could tune the oxidation state of the A site, which may be favorable to electrocatalysts.<sup>8</sup> In some cases, like type I-B, A is not a stable catalytic site in the reaction, such as  $\text{A}^{\delta+}$  in electroreduction reactions. A can downgrade to  $\text{A}^-$  and thus become inactive. Here, by converting B to  $\text{B}^-$ , B could be used as a sacrificing component. Typically, through electro-transfer between A and B, A could be more stable, and the catalytic reaction can continue at an ideal rate, which is important for the activation and transformation of inert bonds. In the following section, recent advances in multicomponent electrocatalysts with one active site and a secondary component that could enhance and stabilize the main component in the electroreduction of  $\text{CO}_2$ ,  $\text{N}_2$ , and  $\text{NO}_3^-$  will be taken as examples to present the application of this model (Fig. 3 and 4). Type I multicomponent catalysts could be

formed through doping, direct synthesis, and *in situ* phase separation. Compared with traditional immobilized catalysts, type I multicomponent catalysts could not only provide a substrate to active sites, but could also enhance the activity of catalytic sites through the interaction. Type I multicomponent catalysts in electroreduction of small molecules could promote the reactions through enhancing substrate adsorption, stabilizing key intermediates, and inhibiting side reactions (such as the hydrogen evolution reaction, HER).

### 3.1.2 Applications in electrochemical reactions

**3.1.2.1 Type I-A.** As is shown in Fig. 3A, Qiao and co-workers recently reported the electroreduction of  $\text{CO}_2$  to  $\text{C}_2\text{H}_5\text{OH}$  on a multicomponent electrocatalyst containing Ag and CuO.<sup>29</sup> The Ag-modified CuO could achieve the production of  $\text{C}_2\text{H}_5\text{OH}$  at  $326.4 \text{ mA cm}^{-2}$  at  $-0.87 \text{ V vs. RHE}$  with a faradaic efficiency (FE) of 40.8%. The outstanding performance was attributed to the CuO activated by Ag, in which the CuAg alloy could be formed under a reductive potential. The strength of  ${}^*\text{CO}$  (including  ${}^*\text{CO}_{\text{bridge}}$  and  ${}^*\text{CO}_{\text{atop}}$ ) was tuned by the Ag component and thus provided an asymmetric and highly efficient C–C coupling pathway to  $\text{C}_2\text{H}_5\text{OH}$  production. Zhu *et al.* explored the utilization of  $\text{La}_{0.4}\text{Sr}_{0.4}\text{Ti}_{0.9}\text{O}_{3-\delta}$  perovskite oxide socketed with sub-3 nm Cu nanoparticles (LSTr-Cu) for reduction of  $\text{CO}_2$  to  $\text{C}_{2+}$

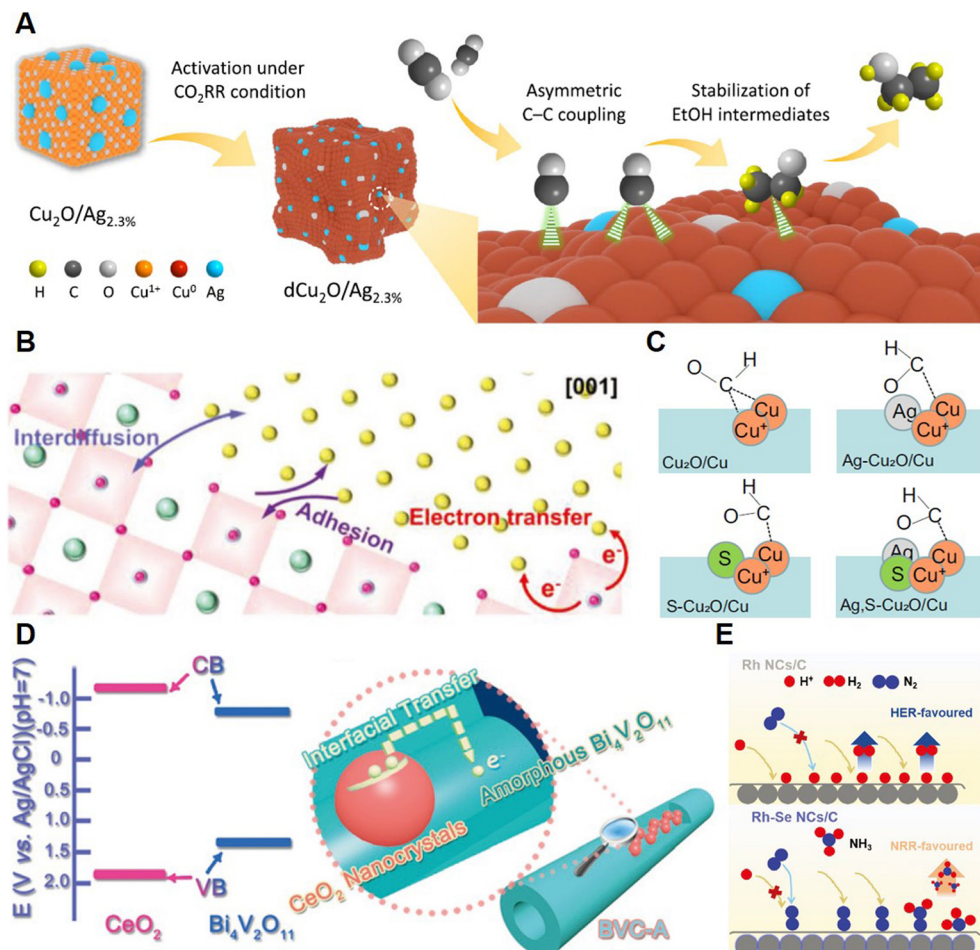


**Fig. 3** (A) Illustration of promoted CO<sub>2</sub>-to-C<sub>2</sub>H<sub>5</sub>OH on a dCu<sub>2</sub>O/Ag<sub>2.3%</sub> electrocatalyst. Reprinted with permission from ref. 29. Copyright 2022, Springer Nature; (B) Interaction between perovskite oxides and Cu nanoparticles. Reprinted with permission from ref. 30. Copyright 2022, John Wiley & Sons, Inc.; (C) \*CHO intermediates on different Cu-based electrocatalysts. Reprinted with permission from ref. 31. Copyright 2022, Springer Nature; (D) Schematic for interfacial charge transfer in BVC-A. Reprinted with permission from ref. 33. Copyright 2018, John Wiley & Sons, Inc.; (E) Different NRR pathways on Rh-based catalysts before and after adding the Se component. Reprinted with permission from ref. 34. Copyright 2020, John Wiley & Sons, Inc.

chemicals.<sup>30</sup> Strong interaction between the perovskite and the Cu component was found to be critical to the enhancement of electrochemical performance (Fig. 3B). During the epitaxial growth, Cu nanoparticles, the active site of the CO<sub>2</sub>RR, could diffuse into the lattice of LStr and thus be tuned by the LStr component by electrotransfer with Ti<sup>4+</sup>/Ti<sup>3+</sup> and the moving d-band center. Compared with the physical mixture of Cu and perovskite, LStr-Cu had enhanced performance for C<sub>2+</sub> production up to 6.2 fold. Our group recently presented an *in situ* dual doping strategy to achieve efficient CO<sub>2</sub>-to-CH<sub>3</sub>OH electrocatalysis with Ag,S-Cu<sub>2</sub>O/Cu, which could achieve a FE of methanol of 67.4% with a current density of 122.7 mA cm<sup>-2</sup> in an H-type cell using an ionic liquid-based electrolyte.<sup>31</sup> The S anion could tune the electronic structure and morphology of the Cu active sites to favor the \*CHO intermediate adsorbed and the CH<sub>3</sub>OH pathway. Besides, the Ag cation could suppress the HER. Their interactions with the Cu active sites could thus enhance the current density and selectivity of the CO<sub>2</sub>RR (Fig. 3C). Wang and co-workers recently reported that Ru sites dispersed on Cu nanowires could catalyze the NITRR at

the industrial-relevant current density of 1 A cm<sup>-2</sup> with a high FE of 93%.<sup>32</sup> The Ru sites were proved to be the catalytic sites of the NITRR while the Cu component could boost the reactivity of the Ru sites through suppressing the HER.

The Yu group reported a noble-metal-free multicomponent electrocatalyst, amorphous phase Bi<sub>4</sub>V<sub>2</sub>O<sub>11</sub>/CeO<sub>2</sub> (BVC-A), for a highly efficient NRR.<sup>33</sup> Significant defects on Bi<sub>4</sub>V<sub>2</sub>O<sub>4</sub> could play a role as active sites, while CeO<sub>2</sub> could serve as the trigger for the formation of the amorphous phase. More importantly, as is shown in Fig. 3D, interfacial electron transfer from CeO<sub>2</sub> to Bi<sub>4</sub>V<sub>2</sub>O<sub>4</sub> enabled by type I band alignment established in the BVC-A catalyst could boost its NRR performance remarkably since the average yield of NH<sub>3</sub> could reach 23.21 mg h<sup>-1</sup> mg<sub>cat</sub><sup>-1</sup> with a FE of 10.16%, which is 3 times better than that of the Bi<sub>4</sub>V<sub>2</sub>O<sub>11</sub>/CeO<sub>2</sub> hybrid with a crystalline phase. Huang *et al.* recently utilized a surface chalcogenation strategy to build multicomponent catalysts with Rh-Se nanocrystals (Rh-Se NCs) which thus promoted the NRR performance.<sup>34</sup> Surface chalcogenation could boost the performance of Rh-Se NCs by reducing the apparent activation energy of reactant molecules and inhibiting the

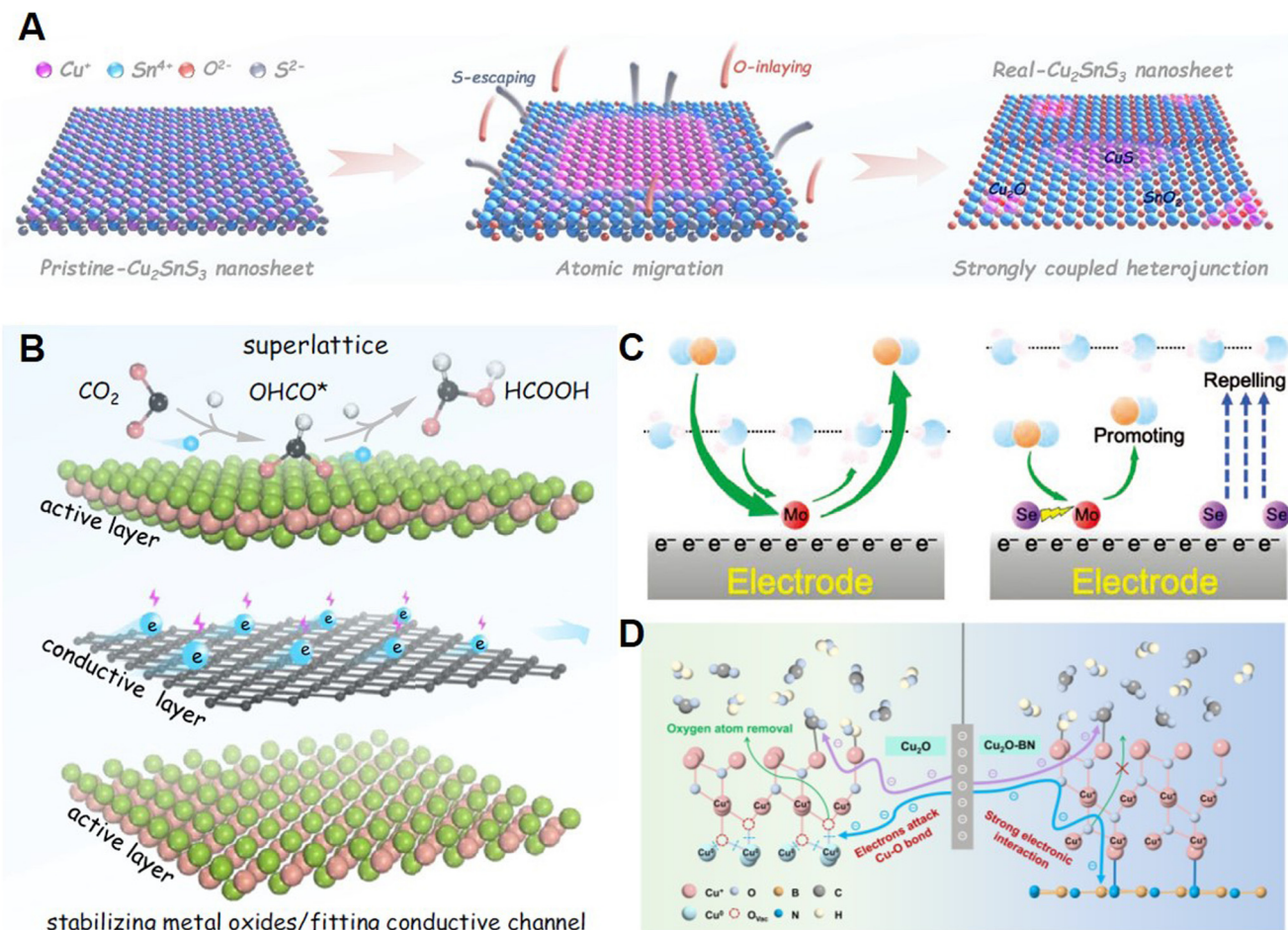


**Fig. 4** (A) Schematic for the *in situ* phase separation of Cu<sub>2</sub>SnS<sub>3</sub> to SnO<sub>2</sub>@CuS and SnO<sub>2</sub>@Cu<sub>2</sub>O heterojunctions with enhanced performance. Reprinted with permission from ref. 35. Copyright 2021, John Wiley & Sons, Inc.; (B) Illustration of a multicomponent superlattice constructed from a metal oxide layer and a conductive layer. Reprinted with permission from ref. 36. Copyright 2022, Springer Nature; (C) Reaction pathway of the CO<sub>2</sub>RR on the Mo-Se multicomponent electrocatalyst. Reprinted with permission from ref. 37. Copyright 2022, John Wiley & Sons, Inc.; (D) Cu active sites protected by strong electronic interaction during the CO<sub>2</sub>RR. Reprinted with permission from ref. 38. Copyright 2022, John Wiley & Sons, Inc.

HER (Fig. 3E). A rather low valence state was constructed for the critical redox inversion induced by the multicomponent core-shell structure of Rh-Se NCs, which could boost the FE by 15 times to 13.3% with an NH<sub>3</sub> yield of 175.6 mg h<sup>-1</sup> g<sub>Rh</sub><sup>-1</sup>.

**3.1.2.2 Type I-B.** Zhai and coworkers reported the construction of SnO<sub>2</sub>@CuS and SnO<sub>2</sub>@Cu<sub>2</sub>O heterojunctions through *in situ* structure evolution of Cu<sub>2</sub>SnS<sub>3</sub> nanosheets as an efficient electrocatalyst for CO<sub>2</sub>-to-HCOOH, with Sn<sup>4+</sup> as the active site, as is presented in Fig. 4A. Sn<sup>4+</sup> was well protected by the electro-self-flow to Cu<sup>+</sup> during electrolysis.<sup>35</sup> The delocalization of Sn-based active sites enabled by charge transfer could boost the coupling between H\* and HCOO\*, thereby accelerating the kinetics of the CO<sub>2</sub>RR and exhibiting excellent electrochemical performance of 83.4% HCOOH formation in a wide potential range (-0.6 V to -1.1 V). The Zhai group also reported a tangible superlattice (Fig. 4B) consisting of two sublayers including [Bi<sub>2</sub>O<sub>2</sub>]<sup>2+</sup> and [Cu<sub>2</sub>Se<sub>2</sub>]<sup>2-</sup> for the protection of Bi active sites in the [Bi<sub>2</sub>O<sub>2</sub>]<sup>2+</sup> layer with the conductive [Cu<sub>2</sub>Se<sub>2</sub>]<sup>2-</sup> sublayer.<sup>36</sup> Compared to the self-reduced Bi metal, the Bi active sites in the [Bi<sub>2</sub>O<sub>2</sub>]<sup>2+</sup> layer

could accept electrons rapidly transferring from the [Cu<sub>2</sub>Se<sub>2</sub>]<sup>2-</sup> layer and be protected in the CO<sub>2</sub>RR. Moreover, in the [Bi<sub>2</sub>O<sub>2</sub>]<sup>2+</sup> layer, Bi p orbitals and O p orbitals were proved to have unique overlaps by theoretical calculations that could enhance the adsorption of the OCHO\* intermediate. Hence, in a wide potential range from -0.4 to -1.1 V, BiCuSeO superlattices could exhibit ideal FE to HCOOH of >90%. Chen and co-workers recently demonstrated a Mo-Se dual single-atom electrocatalyst (MoSA-SeSA) for the CO<sub>2</sub>RR producing CO at a wide potential of -0.4 to -1.0 V with a FE of >90%.<sup>37</sup> As is presented in Fig. 4C, MoSA was proved to be the active site here since it could interact with CO<sub>2</sub> and its intermediates during the CO<sub>2</sub>RR, while SeSA could promote the performance of MoSA. Operando and theoretical studies revealed that SeSA could tune the electronic structure *via* long-range electro-delocalization, which is essential to avoid the inhibition of MoSA caused by the strong CO adsorption. Additionally, SeSA could also suppress the HER through repelling H<sub>2</sub>O molecules and accelerate the CO<sub>2</sub> transport for MoSA to boost the CO<sub>2</sub>RR. Yan and co-workers utilized hexagonal boron nitride (h-BN) nanosheets to decorate Cu<sub>2</sub>O



nanoparticles with  $\text{Cu}^+$  active sites with enhanced stability.<sup>38</sup> Through using the h-BN substrate, the  $\text{C}_2\text{H}_4/\text{CO}$  ratio in the  $\text{CO}_2\text{RR}$  could be improved 1.62 times in contrast to traditional  $\text{Cu}_2\text{O}$  catalysts. As presented in Fig. 4D, interaction in the multicomponent catalysts is critical to performance improvement. The h-BN substrate could strengthen the Cu-O bond and receive partial electron density from  $\text{Cu}_2\text{O}$ . As a result, the  $\text{Cu}^+$  species could be stabilized through its interaction with h-BN during long-term  $\text{CO}_2\text{RR}$ . Zhu and colleagues developed a novel framework by assembling  $[\text{Zr}_{48}\text{Ni}_6]$  nano-cages, which could extract  $\text{AuCl}_4^-$  from electronic waste, due to its high surface area and high stability in solvents.<sup>39</sup> More importantly, this kind of framework adsorbing  $\text{AuCl}_4^-$  could be converted to efficient multicomponent catalysts loading low-cost Au nanoparticles with controlled sizes. The catalysts could exhibit excellent FE of CO as high as 95.2% at a current density of  $102.9 \text{ mA cm}^{-2}$ , which could be attributed to the confinement effect provided by the nanoclusters of  $[\text{Zr}_{48}\text{Ni}_6]$  protecting Au nanoparticles from deactivation. Recently, our group discovered an *in situ* periodic regeneration method to develop long-term stable electrocatalysts for the  $\text{CO}_2\text{RR}$ .<sup>40</sup> A positive potential pulse with a short period was utilized to generate  $\text{Cu}^+$  active sites through the interaction with an electrolyte containing halide ions. The halide anion participated in the formation and stabilization of the highly active catalysts. This method could enhance the performance of the  $\text{CO}_2\text{RR}$  on commercial Cu-based catalysts with a FE of 81.2% and a current density of  $22.7 \text{ mA cm}^{-2}$  with a stability of more than 36 h.

### 3.2 Type II multicomponent catalysts

**3.2.1 Models of multicomponent catalysts.** In type II multicomponent catalysts, two components could participate in the catalytic reaction at the same time providing active intermediates for the conversion of substrate molecules. Specifically, type II-A could supply different intermediates for product formation. For example, although the HER is the main side reaction of most small molecule electroreduction reactions and needs to be suppressed, active proton species play an important role in the electroreduction of small molecules since water could serve as the green proton source in the aqueous system. However, it is difficult for traditional monocomponent catalysts to generate several types of species at the same time. Multicomponent catalysts are thus demanded to generate various intermediates in the reactions. In the  $\text{CO}_2\text{RR}$ , reactive hydrogen species could enhance the conversion of  $\text{CO}_2$  to value-added products with multiple electron transfer processes such as alcohols. In addition, reactive hydrogen species are also very important for the electrochemical hydrogenation of inert bonds in  $\text{N}_2$ . Type II-B catalysts could simultaneously produce the same product, thus improving the performance of the reaction. In multicomponent catalysts, the synergistic effect of each

component has been widely studied and proved to promote the reaction, making the performance of the multicomponent catalysts better than the effect of the two components acting separately. Additionally, the interaction between the loaded component and the substrate is also very important in this type of multicomponent catalyst. In the traditional impregnated catalysts, the substrate could not provide active sites, while recent studies showed that the activity of the catalyst substrates could boost the electroreduction efficiently. Hence, type II multicomponent catalysts could drive the electroreduction of small molecules with enhanced efficiency and produce more valuable products, which would be introduced in detail in the next subsection.

#### 3.2.2 Applications in electrochemical reactions

**3.2.2.1 Type II-A.** Our group reported the efficient conversion of  $\text{CO}_2$  to methanol on Mo-Bi bimetallic chalcogenide (MBC) in ionic liquid-based electrolytes through synergistic effects confirmed by control experiments. CO and  $\text{H}_2$  intermediates were generated at Bi and Mo sites, respectively, and these intermediates were proved to be important in the production of methanol. The FE of methanol on MBC catalysts could reach 71.2% with a current density of  $12.1 \text{ mA cm}^{-2}$ .<sup>41</sup> Guo and co-workers recently reported phthalocyanines polymerized through the solid ion thermal utilizing Scholl reaction (Fig. 5A) with carbon nanotubes as the substrates, which could provide both  $\text{CoN}_4$  sites and  $\text{H}_2\text{Pc}$  sites for the  $\text{CO}_2\text{RR}$ .<sup>42</sup> As is shown in Fig. 5B, in the phthalocyanine catalysts,  $\text{CoN}_4$  could serve as the active site to interact with  $\text{CO}_2$  molecules while  $\text{H}_2\text{Pc}$  sites could boost the  $\text{CO}_2\text{RR}$  as the donors of protons and electrons. As a result, the performance of phthalocyanines could reach a FE of 97% with a large current density of  $>200 \text{ mA cm}^{-2}$ . Sargent *et al.* explored the doping of hydroxide and oxide to Cu catalysts that could tune the adsorption energy of hydrogen species on the Cu surface through the synthesis of  $\text{Ce}(\text{OH})_x$ -doped-Cu catalysts.<sup>43</sup> As is presented in Fig. 5C, hydroxide and oxide dopants could enhance the hydrogenation of  $^*\text{HCOOH}$  to produce ethanol products by providing proton intermediates. Competently,  $\text{Ce}(\text{OH})_x$ -doped-Cu catalysts could reach an ethanol partial current density of  $128 \text{ mA cm}^{-2}$  with a FE of 43% and a high ethanol/ethylene ratio. The Cheng group reported a nanoporous NiSb alloy as an efficient multicomponent catalyst for the NRR.<sup>44</sup> As is presented in Fig. 5D, the Ni sites could enhance the hydrogenation of  $\text{N}_2$  and the Sb sites could separate the active sites for  $\text{N}_2$  adsorption and active proton species generation, which is helpful to the activation of inert  $\text{N}_2$  molecules. Due to the separated active sites, the NRR performance on the NiSb alloy could reach a high  $\text{NH}_3$  yield rate of  $56.9 \text{ } \mu\text{g h}^{-1} \text{ mg}^{-1}$  with a FE of 48.0%.

**3.2.2.2 Type II-B.** Recently, defective CuO-supported atomic Sn sites were synthesized as superior electrocatalysts for  $\text{CO}_2$ -to- $\text{CH}_3\text{OH}$  transformation aided by the cooperation of multiple sites including Sn, oxygen vacancies, and the CuO

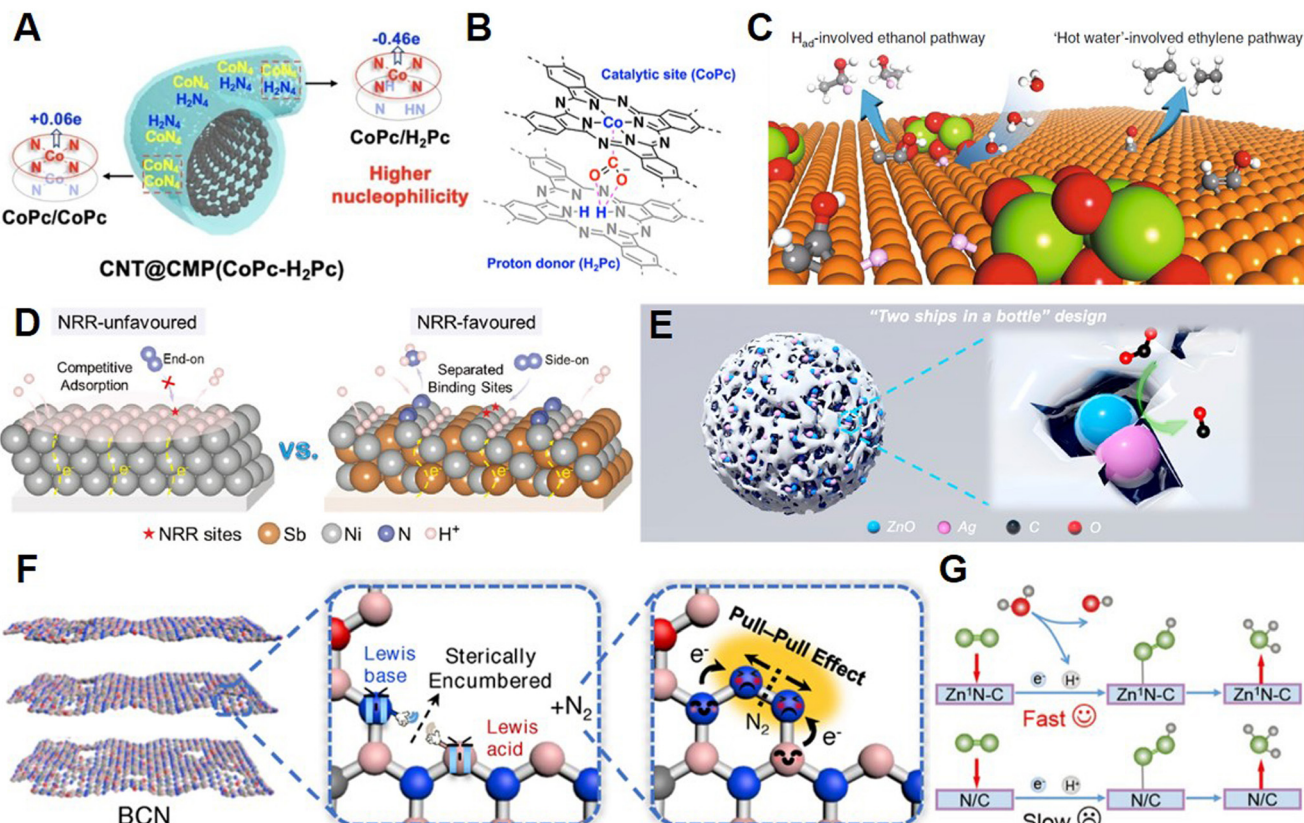


**Fig. 5** (A) Structure and (B) catalytic mechanism of the CNT@CMP(CoPc-H<sub>2</sub>Pc) electrocatalyst. Reprinted with permission from ref. 42. Copyright 2022, John Wiley & Sons, Inc.; (C) Proton-involved CO<sub>2</sub>-to-CH<sub>2</sub>H<sub>5</sub>OH pathway on the Ce(OH)<sub>x</sub>-doped-Cu electrocatalyst. Reprinted with permission from ref. 43. Copyright 2019, Springer Nature; (D) Comparison of the NRR on different Ni-based catalysts. Reprinted with permission from ref. 44. Copyright 2021, John Wiley & Sons, Inc.; (E) “Two ships in a bottle” design strategy of Zn-Ag-O catalysts for the CO<sub>2</sub>RR. Reprinted with permission from ref. 46. Copyright 2021, the American Chemical Society; (F) Advantages of BCN with frustrated Lewis pairs in the NRR. Reprinted with permission from ref. 48. Copyright 2022, John Wiley & Sons, Inc.; (G) Comparison of NRR pathways on Zn<sup>1</sup>N-C and N/C. Reprinted with permission from ref. 49. Copyright 2022, John Wiley & Sons, Inc.

support, which could generate CH<sub>3</sub>OH at the same time.<sup>45</sup> As a result, the multicomponent catalyst could exhibit a methanol FE of 88.6% with a current density of 67.0 mA cm<sup>-2</sup>. In Fig. 5E, Chen and colleagues proposed a “two ships in a bottle” design and synthesized a multicomponent Zn-Ag-O catalyst for the CO<sub>2</sub>RR with a high energy efficiency of 60.9%, a CO FE of 94.1%, and ideal stability.<sup>46</sup> The excellent performance of Zn-Ag-O could be attributed to the enhanced adsorption of \*COOH intermediates on the surface of Zn and Ag domains. Additionally, the surfaces could also hinder the detachment and agglomeration of catalysts during the CO<sub>2</sub>RR. The unique porous structure in metal-organic frameworks could provide a useful platform for multicomponent catalysts.<sup>47</sup> Zhu and co-workers reported a porous 3D In-MOF,  $\{(\text{Me}_2\text{NH}_2)[\text{In}(\text{BCP})]\cdot2\text{DMF}\}_n$  (V11), with two types of channels that could transfer CO<sub>2</sub> to HCOOH with a FE of 76%.<sup>44</sup> Researchers discovered that carbon particles produced from methylene blue molecules could be introduced to the channels of V11 through pyrolysis. Multicomponent catalysts containing V11 and carbon particles could improve both the FE (from 76.0% to 90.1%) and current density (2.2 times) of HCOOH generation, because of the enhanced charge and mass transfer and sufficiently exposed active sites. The Dai group presented a

defective boron carbon nitride (BCN) catalyst with both Lewis acid and base sites for the NRR, which has long-term stability and could exhibit a high FE of 18.9%, and the yield of NH<sub>3</sub> could reach 20.9  $\mu\text{g h}^{-1} \text{mg}_{\text{cat}}^{-1}$ .<sup>48</sup> The frustrated Lewis pairs (FLPs) in BCN catalysts could provide the possibility for the formation of a six-membered ring intermediate during the NRR, as is shown in Fig. 5F, enabling the efficient N<sub>2</sub> cleavage through pull-pull efficiency. Hou and collaborators reported hollow porous N-doped carbon nanofibers anchoring single Zn(i) sites (Zn<sup>1</sup>N-C) for the NRR.<sup>49</sup> As is presented in Fig. 5G, the isolated Zn sites and nearby graphitic N sites could synergistically activate and convert the inert N<sub>2</sub> molecules by decreasing the energy barrier of the \*NNH intermediate formation, which was proved to be the rate-limiting step in the NRR. Therefore, the yield of NH<sub>3</sub> production on Zn<sup>1</sup>N-C could reach 16.1  $\mu\text{g h}^{-1} \text{mg}_{\text{cat}}^{-1}$  with a FE of 11.8%. The Zhang group demonstrated a highly efficient NITRR on a multicomponent Cu/Cu<sub>2</sub>O catalyst *in situ* derived from CuO with a FE as high as 95.8% and an excellent selectivity of 82%.<sup>50</sup> Electron transfer from Cu<sub>2</sub>O to Cu led to \*NOH intermediate adsorption at the interface, which was attributed to the promoted NH<sub>3</sub> production and suppressed HER.



### 3.3 Type III multicomponent catalysts

**3.3.1 Models of multicomponent catalysts.** The type III multicomponent catalysts emphasize the sequential action of different catalytic sites in the electroreduction of small molecules. For example, type III-A multicomponent catalysts could convert the substrate molecules in tandem with the migration of intermediates. Each active site could catalyze the individual step in the reaction, which could be coupled into the whole reaction. This effect is important because of the ability to boost key processes in the electroreduction of small molecules such as  $C_2+$  product generation from *in situ* generated CO intermediates and efficient hydrogenation of  $NO_2^-$  intermediates in the NITRR to produce  $NH_3$  with an enhanced yield rate. The catalytic sites with different components could provide active sites for the above-mentioned steps. Materials including alloys, bimetallic

heterostructures, and framework materials could serve as efficient catalysts for this subtype of catalyst. In type III-B, active sites could also boost the reaction with the help of components that could enhance the adsorption of substrate molecules such as  $CO_2$ ,  $N_2$ , and  $NO_3^-$ . These substrates usually suffer from low solubility and (or) concentration in the electrolyte, which could hinder their electroreduction with the limitation of mass transfer. Thus, the component in the catalysts that could provide high local concentration through adsorption could assist in the promotion of electrochemical performance of real active sites fed with more substrates. Porous materials, which could provide ideal gas adsorption due to their high specific surface area, were proved to be effective providers of adsorption sites in type III-B catalysts. In addition, catalysts with unique electric fields and nanostructures were also reported.

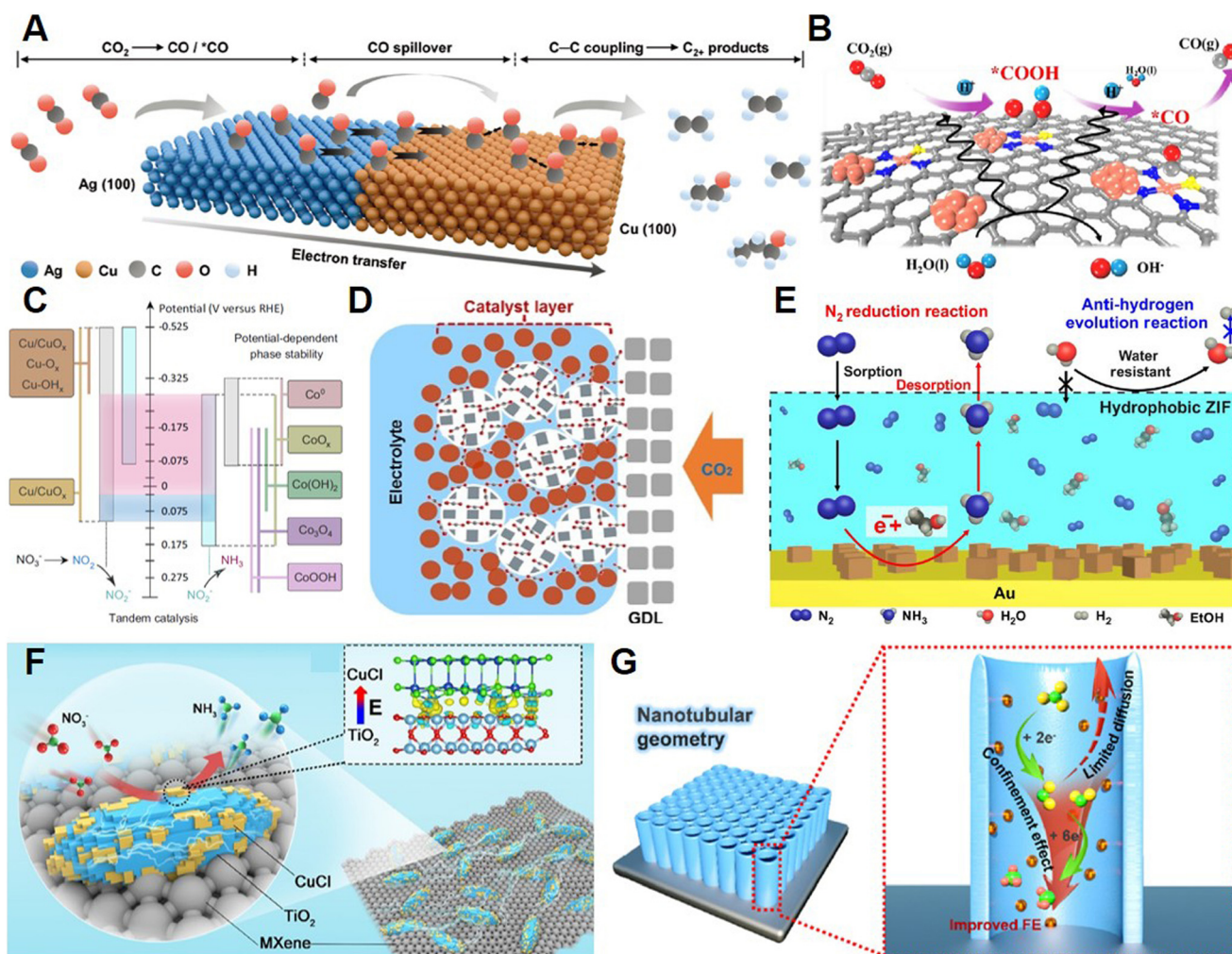


**Fig. 6** (A) Proposed reaction mechanism for production of  $C_2$  molecules on the  $Ag_{65}-Cu_{35}$  JNS-100 catalyst. Reprinted with permission from ref. 51. Copyright 2022, John Wiley & Sons, Inc.; (B) Tandem  $CO_2$ -to- $CO$  transformation pathway through  $Cu-S_1N_3/Cu_x$ . Reprinted with permission from ref. 52. Copyright 2021, John Wiley & Sons, Inc.; (C) Intermediates and their conversion over the  $CuCoSP$  tandem catalyst during the  $NO_3RR$ . Reprinted with permission from ref. 55. Copyright 2022, Springer Nature; (D)  $CO_2$  diffusion in GDE enhanced by CC3. Reprinted with permission from ref. 56. Copyright 2022, John Wiley & Sons, Inc.; (E)  $N_2$  diffusion on the surface of catalysts encapsulated with ZIF. Reprinted with permission from ref. 57. Copyright 2018, American Association for the Advancement of Science; (F) Built-in electric field in  $CuCl$ -BEF catalysts enabling enhanced NITRR. Reprinted with permission from ref. 58. Copyright 2021, John Wiley & Sons, Inc.; (G) Illustration of the nanoreactor for NITRR with enhanced FE. Reprinted with permission from ref. 59. Copyright 2022, Elsevier.



### 3.3.2 Applications in electrochemical reactions

**3.3.2.1 Type III-A.** Fan and collaborators demonstrated the delicate synthesis of Ag–Cu Janus nanocatalysts ( $\text{Ag}_{65}\text{-Cu}_{35}$  JNS-100) that could reduce  $\text{CO}_2$  to  $\text{C}_{2+}$  products.<sup>51</sup> As is shown in Fig. 6A,  $\text{CO}_2$  could transfer to CO on the Ag sites, followed by the CO spillover and dimerization on the Cu component. Compared with Cu nanocubes,  $\text{Ag}_{65}\text{-Cu}_{35}$  JNS-100 could exhibit enhanced FE of  $\text{C}_{2+}$  products. The Yu group demonstrated a tandem catalyst for  $\text{CO}_2$ -to-CO through anchoring single atomic Cu sites and Cu nanoclusters on the carbon support doped with N and S.<sup>52</sup> The catalyst ( $\text{Cu-S}_1\text{N}_3$ ) could exhibit a CO FE of 100% under optimized conditions, which was attributed to the generation of  $^*\text{CO}_2^-$  intermediates on  $\text{CuN}_4$  sites and the hydrogenation of  $^*\text{CO}_2^-$  on Cu clusters (Fig. 6B). Bao and coworkers reported the  $\text{CO}_2$ -RR producing  $\text{CH}_4$  using copper-free catalysts consisting of phthalocyanine (CoPc) and zinc–nitrogen–carbon (Zn–N–C) sites, which had much better performance than catalysts with one type of site alone.<sup>53</sup>  $\text{CO}_2$  was proved to be reduced to CO on the CoPc sites, while *in situ* generated CO could be fed to Zn–N–C sites as substrates to produce  $\text{CH}_4$ . Recently, Wu and coworkers reported that segmented gas-diffusion electrodes (s-GDEs) with multiple components could enhance the conversion of  $\text{CO}_2$  to  $\text{C}_{2+}$  chemicals through the prolonged residence time of CO intermediates enabled by the segment at the inlet.<sup>54</sup> The Ag component could transfer  $\text{CO}_2$  to CO, while Cu sites could utilize the *in situ* generated CO intermediates diffused from the surface of Ag to produce the  $\text{C}_{2+}$  products through the formation of C–C coupling. Based on this strategy that could increase the yield of both CO intermediates and  $\text{C}_{2+}$  fine products at the same time, researchers developed a Cu/Fe–N–C s-GDE, which could exhibit a high partial current density of  $\text{C}_{2+}$  production of  $\sim 1 \text{ A cm}^{-2}$  with a FE of 90%. The Schuhmann lab demonstrated a tandem catalyst for  $\text{NH}_3$  synthesis from  $\text{NO}_3^-$  with a core–shell catalyst with Cu/CuO<sub>x</sub> and Co/CoO phases.<sup>55</sup> As is presented in Fig. 6C,  $\text{NO}_3^-$  could first be reduced on the Cu-based sites to  $\text{NO}_2^-$ , while  $\text{NH}_3$  could be generated from  $\text{NO}_2^-$  on the surface of Co sites. The high local concentration of  $\text{NO}_2^-$  provided by Cu sites could boost the yield of  $\text{NH}_3$  production obviously. Consequently, a high yield of  $\text{NH}_3$  of  $1.17 \text{ mmol cm}^{-2} \text{ h}^{-1}$  could be reached on the multicomponent catalysts with a tandem reduction.

**3.3.2.2 Type III-B.** Recently, our group reported porous organic cages (POCs) as an additive for the  $\text{CO}_2$ RR on Cu catalysts since the limited solubility of  $\text{CO}_2$  in aqueous solution could hinder the mass transfer and thus reduce the performance.<sup>56</sup>  $\text{CO}_2$  could be adsorbed in the pores of POCs, followed by its diffusion to the surface of Cu catalytic sites. Compared with the  $\text{CO}_2$  diffusion from an aqueous electrolyte, it was more favorable to diffuse from the hydrophobic pores of the POCs. The enhanced attachment between  $\text{CO}_2$  and the Cu surface enabled the enhanced  $\text{CO}_2$ RR performance and decreased the HER. As a result, the FE of  $\text{C}_{2+}$  chemicals on Cu modified with CC3 (one of the POCs) could reach 76% with a high current density of  $1.7 \text{ A}$

$\text{cm}^{-2}$ . Ling and coworkers designed a reticular chemistry approach for selective NRR, in which zeolitic imidazolate framework-71 (ZIF) was introduced to the surface of NRR electrocatalysts (Fig. 6D).<sup>57</sup> The multicomponent catalysts could enhance the interactions between  $\text{N}_2$  molecules and active sites, while the HER could be suppressed. The catalysts coated with ZIF could exhibit a selectivity to  $\text{NH}_3$  of  $\sim 90\%$  and an enhanced FE of 11%. The Lu group synthesized a multicomponent catalyst *via* stacking CuCl and TiO<sub>2</sub> on an MXene substrate (CuCl\_BEF), which had a built-in electric field because of the electron transfer from TiO<sub>2</sub> to CuCl.<sup>58</sup> The unique built-in electric field could assist the accumulation of  $\text{NO}_3^-$  around TiO<sub>2</sub> sites with positive charge and produce a high local  $\text{NO}_3^-$  concentration to the Cu catalytic sites (Fig. 6E). Therefore, the electrochemical production of  $\text{NH}_3$  on CuCl\_BEF could reach a selectivity of 98.6% and a high yield of  $64.4 \text{ h}^{-1}$  in low  $\text{NO}_3^-$  concentration electrolyte ( $100 \text{ mg L}^{-1}$ ). Recently, Li and colleagues demonstrated a multicomponent catalyst consisting of CuO<sub>x</sub> active sites and a TiO<sub>2</sub> nanotube reactor (TiO<sub>2</sub> NTs/CuO<sub>x</sub>) for the NITRR, in which TiO<sub>2</sub> could hinder the diffusion of  $\text{NO}_2^-$  by-products and thus boost the reduction of  $\text{NO}_2^-$  on CuO<sub>x</sub> sites and produce  $\text{NH}_3$  with higher selectivity.<sup>59</sup> The maximum FE of the NITRR on TiO<sub>2</sub> NTs/CuO<sub>x</sub> could reach 92.23% and a high  $\text{NH}_3$  yield rate of  $1241.81 \text{ } \mu\text{g h}^{-1} \text{ cm}^{-2}$  could be achieved.

## 4 Summary and outlook

As discussed above, the electrochemical reduction of small molecules on multicomponent catalysts could contribute to the carbon neutrality and sustainability goals of our society through producing value-added chemicals with renewable sources, and is substantially becoming a crucial research area. However, large-scale and industrial applications of these emerging electrochemical reactions such as the  $\text{CO}_2$ RR, NRR, and NITRR have not been realized to date, which is caused by their low energy efficiency, high cost, and unsatisfactory economic benefits. Additionally, some essential scientific and technological issues need to be addressed in the future, some of which are highlighted as follows:

First, there is no doubt that synthesizing multicomponent electrocatalysts with high reaction activity, ideal selectivity, long-term stability, and low cost is a long-range objective for researchers to advance the electroreduction of small molecules to industry. For instance, the reduction of  $\text{CO}_2$  to long-chain organic chemicals is also important, which is proposed to be promoted by multicomponent catalysts. Additionally, reduction of  $\text{CO}_2/\text{N}_2$  with low partial pressure or undesired impurities and  $\text{NO}_x^-$  at low concentration would be enabled by multicomponent catalysts. On the other hand, more research should be conducted to study the structure–property relationship and the interaction of different components in these catalysts.

Second, electrolytes are also an important unit in the electrochemical reduction of small molecules besides catalysts, which could be designed together toward an efficient electrolyte–catalyst system.<sup>60</sup> The rules in the coupling of electrolytes and catalysts for electrochemical transformation are needed to be explored.

Third, compared with the direct electroreduction of small molecules with water, few research studies have been conducted on the co-reduction of these molecules and their electrochemical coupling with other organic compounds. Recently, electrochemical synthesis of carboxylic acid, carbonate, urea, amine, and other organic chemicals from the electroreduction of small molecules was reported, but these reactions are still in the starting stage.<sup>61–67</sup> Multicomponent catalysts have the advantages of producing C–N-containing intermediates simultaneously and promoting the C–N coupling.<sup>68</sup> Hence, more attention should be paid to developing new routes for electrochemical synthesis using multicomponent catalysts.

Fourth, the electroreduction of small molecules is very complex and our current knowledge is very limited to understand the reaction mechanism of these reactions in detail.<sup>69,70</sup> As a result, *in situ* characterization and theoretical studies should be combined to provide more understanding of the mechanism.

Fifth, we believe that, in the near future, industrial electroreduction of small molecules should be realized, and some problems should be solved including energy harvesting devices, efficient adsorption of substrates such as CO<sub>2</sub>, advanced flow electrolyzers, coupled reactions, and product separation.

## Conflicts of interest

The authors declare no conflict of interest.

## Acknowledgements

This work was supported by the National Natural Science Foundation of China (22002172 and 22121002), the Beijing Natural Science Foundation (J210020) and the Photon Science Center for Carbon Neutrality.

## References

- 1 M. He, Y. Sun and B. Han, Green carbon science: Scientific basis for integrating carbon resource processing, utilization, and recycling, *Angew. Chem., Int. Ed.*, 2013, **52**, 9620–9633.
- 2 M. He, Y. Sun and B. Han, Green carbon science: Efficient carbon resource processing, utilization, and recycling towards carbon neutrality, *Angew. Chem., Int. Ed.*, 2022, **61**, e202112835.
- 3 P. Gao, L. Zhong, B. Han, M. He and Y. Sun, Green carbon science: Keeping the pace in practice, *Angew. Chem., Int. Ed.*, 2022, **61**, e202210095.
- 4 S. Jia, X. Ma, X. Sun and B. Han, Electrochemical transformation of CO<sub>2</sub> to value-added chemicals and fuels, *CCS Chem.*, 2022, **4**, 3213–3229.
- 5 X. Song, S. Jia, L. Xu, J. Feng, L. He, X. Sun and B. Han, Towards sustainable CO<sub>2</sub> electrochemical transformation via coupling design strategy, *Mater. Today Sustain.*, 2022, **19**, 100179.
- 6 L. Wu, W. Guo, X. Sun and B. Han, Rational design of nanocatalysts for ambient ammonia electrosynthesis, *Pure Appl. Chem.*, 2021, **93**, 777–797.
- 7 Y. Kawamata and P. S. Baran, Electrosynthesis: Sustainability is not enough, *Joule*, 2020, **4**, 701–704.
- 8 X. Tan, X. Sun and B. Han, Ionic liquid-based electrolytes for CO<sub>2</sub> electroreduction and CO<sub>2</sub> electroorganic transformation, *Natl. Sci. Rev.*, 2021, **9**, nwab022.
- 9 X. Song, W. Guo, X. Ma, L. Xu, X. Tan, L. Wu, S. Jia, T. Wu, J. Ma, F. Zhang, J. Jia, X. Sun and B. Han, Boosting CO<sub>2</sub> electroreduction over Co nanoparticles supported on N, B-co-doped graphitic carbon, *Green Chem.*, 2022, **24**, 1488–1493.
- 10 X. Tan, W. Guo, S. Liu, S. Jia, L. Xu, J. Feng, X. Yan, C. Chen, Q. Zhu, X. Sun and B. Han, A Sn-stabilized Cu<sup>8+</sup> electrocatalyst toward highly selective CO<sub>2</sub>-to-CO in a wide potential range, *Chem. Sci.*, 2022, **13**, 11918.
- 11 Y. Xu, H. Yang, X. Chang and B. Xu, Introduction to electrocatalytic kinetics, *Acta Phys.-Chim. Sin.*, 2022, **39**, 2210025.
- 12 J. Shi, On the synergistic catalytic effect in heterogeneous nanocomposite catalysts, *Chem. Rev.*, 2013, **113**, 2139–2181.
- 13 L. Zhou and R. Lv, Rational catalyst design and interface engineering for electrochemical CO<sub>2</sub> reduction to high-valued alcohols, *J. Energy Chem.*, 2022, **70**, 310–331.
- 14 Y. Zhai, P. Han, Q. Yun, Y. Ge, X. Zhang, Y. Chen and H. Zhang, Phase engineering of metal nanocatalysts for electrochemical CO<sub>2</sub> reduction, *eScience*, 2022, **2**, 467–485.
- 15 D. D. Zhu, J. L. Liu and S. Z. Qiao, Recent Advances in Inorganic Heterogeneous Electrocatalysts for Reduction of Carbon Dioxide, *Adv. Mater.*, 2016, **28**, 3423–3452.
- 16 S. Jin, Z. Hao, K. Zhang, Z. Yan and J. Chen, Advances and challenges for the electrochemical reduction of CO<sub>2</sub> to CO: From fundamentals to industrialization, *Angew. Chem., Int. Ed.*, 2021, **60**, 20627–20648.
- 17 H. Shin, K. U. Hansen and F. Jiao, Techno-economic assessment of low-temperature carbon dioxide electrolysis, *Nat. Sustain.*, 2021, **4**, 911–919.
- 18 F. Chang, G. Zhan, Z. Wu, Y. Duan, S. Shi, S. Zeng, X. Zhang and S. Zhang, Technoeconomic Analysis and Process Design for CO<sub>2</sub> Electroreduction to CO in Ionic Liquid Electrolyte, *ACS Sustainable Chem. Eng.*, 2021, **9**, 9045–9052.
- 19 M. Jouny, W. Luc and F. Jiao, General Techno-Economic Analysis of CO<sub>2</sub> Electrolysis Systems, *Ind. Eng. Chem. Res.*, 2018, **57**, 2165–2177.
- 20 M. G. Kibria, J. P. Edwards, C. M. Gabardo, C.-T. Dinh, A. Seifitokaldani, D. Sinton and E. H. Sargent, Electrochemical CO<sub>2</sub> Reduction into Chemical Feedstocks: From Mechanistic Electrocatalysis Models to System Design, *Adv. Mater.*, 2019, **31**, 1807166.
- 21 T. Xu, B. Ma, J. Liang, L. Yue, Q. Liu, T. Li, H. Zhao, Y. Luo, S. Lu and X. Sun, Recent Progress in Metal-Free Electrocatalysts



toward Ambient N<sub>2</sub> Reduction Reaction, *Acta Phys.-Chim. Sin.*, 2021, **37**, 2009043.

22 Y. Wan, J. Xu and R. Lv, Heterogeneous electrocatalysts design for nitrogen reduction reaction under ambient conditions, *Mater. Today*, 2019, **27**, 69–90.

23 Y. Wu, Z. Jiang, Z. Lin, Y. Liang and H. Wang, Direct electrosynthesis of methylamine from carbon dioxide and nitrate, *Nat. Sustain.*, 2021, **4**, 725–730.

24 D. Wang, C. Chen and S. Wang, Defect engineering for advanced electrocatalytic conversion of nitrogen-containing molecules, *Sci. China: Chem.*, 2022, DOI: [10.1007/s11426-11022-11419-y](https://doi.org/10.1007/s11426-11022-11419-y).

25 H. Wan, A. Bagger and J. Rossmeisl, Electrochemical Nitric Oxide Reduction on Metal Surfaces, *Angew. Chem., Int. Ed.*, 2021, **60**, 21966–21972.

26 H. Zhang, Y. Li, C. Cheng, J. Zhou, P. Yin, H. Wu, Z. Liang, J. Zhang, Q. Yun, A.-L. Wang, L. Zhu, B. Zhang, W. Cao, X. Meng, J. Xia, Y. Yu and Q. Lu, Isolated electron-rich ruthenium atoms in intermetallic compounds for boosting electrochemical nitric oxide reduction to ammonia, *Angew. Chem., Int. Ed.*, 2022, DOI: [10.1002/anie.202213351](https://doi.org/10.1002/anie.202213351).

27 Y. Zhang, Y. Wang, L. Han, S. Wang, T. Cui, Y. Yan, M. Xu, H. Duan, Y. Kuang and X. Sun, Nitrite electroreduction to ammonia promoted by molecular carbon dioxide with near-unity faradaic efficiency, *Angew. Chem., Int. Ed.*, 2022, DOI: [10.1002/anie.202213711](https://doi.org/10.1002/anie.202213711).

28 S. E. Braley, J. Xie, Y. Losovoj and J. M. Smith, Graphite conjugation of a macrocyclic cobalt complex enhances nitrite electroreduction to ammonia, *J. Am. Chem. Soc.*, 2021, **143**, 7203–7208.

29 P. Wang, H. Yang, C. Tang, Y. Wu, Y. Zheng, T. Cheng, K. Davey, X. Huang and S.-Z. Qiao, Boosting electrocatalytic CO<sub>2</sub>–to–ethanol production via asymmetric C–C coupling, *Nat. Commun.*, 2022, **13**, 3754.

30 Y. Li, F. Liu, Z. Chen, L. Shi, Z. Zhang, Y. Gong, Y. Zhang, X. Tian, Y. Zhang, X. Qiu, X. Ding, X. Bai, H. Jiang, Y. Zhu and J. Zhu, Perovskite-socketed sub-3 nm copper for enhanced CO<sub>2</sub> electroreduction to C<sub>2+</sub>, *Adv. Mater.*, 2022, **34**, 2206002.

31 P. Li, J. Bi, J. Liu, Q. Zhu, C. Chen, X. Sun, J. Zhang and B. Han, In situ dual doping for constructing efficient CO<sub>2</sub>–to–methanol electrocatalysts, *Nat. Commun.*, 2022, **13**, 1965.

32 F.-Y. Chen, Z.-Y. Wu, S. Gupta, D. J. Rivera, S. V. Lambeets, S. Pecaut, J. Y. T. Kim, P. Zhu, Y. Z. Finfrock, D. M. Meira, G. King, G. Gao, W. Xu, D. A. Cullen, H. Zhou, Y. Han, D. E. Perea, C. L. Muñich and H. Wang, Efficient conversion of low-concentration nitrate sources into ammonia on a Ru-dispersed Cu nanowire electrocatalyst, *Nat. Nanotechnol.*, 2022, **17**, 759–767.

33 C. Lv, C. Yan, G. Chen, Y. Ding, J. Sun, Y. Zhou and G. Yu, An amorphous noble-metal-free electrocatalyst that enables nitrogen fixation under ambient conditions, *Angew. Chem., Int. Ed.*, 2018, **57**, 6073–6076.

34 C. Yang, B. Huang, S. Bai, Y. Feng, Q. Shao and X. Huang, A generalized surface chalcogenation strategy for boosting the electrochemical N<sub>2</sub> fixation of metal nanocrystals, *Adv. Mater.*, 2020, **32**, 2001267.

35 W. Wang, Z. Wang, R. Yang, J. Duan, Y. Liu, A. Nie, H. Li, B. Y. Xia and T. Zhai, In situ phase separation into coupled interfaces for promoting CO<sub>2</sub> electroreduction to formate over a wide potential window, *Angew. Chem., Int. Ed.*, 2021, **60**, 22940–22947.

36 J. Duan, T. Liu, Y. Zhao, R. Yang, Y. Zhao, W. Wang, Y. Liu, H. Li, Y. Li and T. Zhai, Active and conductive layer stacked superlattices for highly selective CO<sub>2</sub> electroreduction, *Nat. Commun.*, 2022, **13**, 2039.

37 K. Sun, K. Yu, J. Fang, Z. Zhuang, X. Tan, Y. Wu, L. Zeng, Z. Zhuang, Y. Pan and C. Chen, Nature-inspired design of molybdenum–selenium dual-single-atom electrocatalysts for CO<sub>2</sub> reduction, *Adv. Mater.*, 2022, **34**, 2206478.

38 Y. Zhou, Y. Yao, R. Zhao, X. Wang, Z. Fu, D. Wang, H. Wang, L. Zhao, W. Ni, Z. Yang and Y.-M. Yan, Stabilization of Cu<sup>+</sup> via strong electronic interaction for selective and stable CO<sub>2</sub> electroreduction, *Angew. Chem., Int. Ed.*, 2022, **61**, e202205832.

39 Z.-H. Zhu, Z.-L. Liang, Z.-H. Jiao, X.-L. Jiang, Y. Xie, H. Xu and B. Zhao, A facile strategy to obtain low-cost and high-performance gold-based catalysts from artificial electronic waste by [Zr<sub>48</sub>Ni<sub>6</sub>] nano-cages in MOFs for CO<sub>2</sub> electroreduction to CO, *Angew. Chem., Int. Ed.*, 2022, **61**, e202214243.

40 L. Xu, X. Ma, L. Wu, X. Tan, X. Song, Q. Zhu, C. Chen, Q. Qian, Z. Liu, X. Sun, S. Liu and B. Han, In situ periodic regeneration of catalyst during CO<sub>2</sub> electroreduction to C<sub>2+</sub> products, *Angew. Chem., Int. Ed.*, 2022, **61**, e202210375.

41 X. Sun, Q. Zhu, X. Kang, H. Liu, Q. Qian, Z. Zhang and B. Han, Molybdenum–bismuth bimetallic chalcogenide nanosheets for highly efficient electrocatalytic reduction of carbon dioxide to methanol, *Angew. Chem., Int. Ed.*, 2016, **55**, 6771–6775.

42 R. Wang, X. Wang, W. Weng, Y. Yao, P. Kidkhunthod, C. Wang, Y. Hou and J. Guo, Proton/electron donors enhancing electrocatalytic activity of supported conjugated microporous polymers for CO<sub>2</sub> reduction, *Angew. Chem., Int. Ed.*, 2022, **61**, e202115503.

43 M. Luo, Z. Wang, Y. C. Li, J. Li, F. Li, Y. Lum, D.-H. Nam, B. Chen, J. Wicks, A. Xu, T. Zhuang, W. R. Leow, X. Wang, C.-T. Dinh, Y. Wang, Y. Wang, D. Sinton and E. H. Sargent, Hydroxide promotes carbon dioxide electroreduction to ethanol on copper via tuning of adsorbed hydrogen, *Nat. Commun.*, 2019, **10**, 5814.

44 G. Fan, W. Xu, J. Li, J.-L. Chen, M. Yu, Y. Ni, S. Zhu, X.-C. Su and F. Cheng, Nanoporous NiSb to enhance nitrogen electroreduction via tailoring competitive adsorption sites, *Adv. Mater.*, 2021, **33**, 2101126.

45 W. Guo, S. Liu, X. Tan, R. Wu, X. Yan, C. Chen, Q. Zhu, L. Zheng, J. Ma, J. Zhang, Y. Huang, X. Sun and B. Han, Highly efficient CO<sub>2</sub> electroreduction to methanol through atomically dispersed Sn coupled with defective CuO catalysts, *Angew. Chem., Int. Ed.*, 2021, **60**, 21979–21987.

46 Z. Zhang, G. Wen, D. Luo, B. Ren, Y. Zhu, R. Gao, H. Dou, G. Sun, M. Feng, Z. Bai, A. Yu and Z. Chen, “Two ships in a bottle” design for Zn–Ag–O catalyst enabling selective and



long-lasting CO<sub>2</sub> electroreduction, *J. Am. Chem. Soc.*, 2021, **143**, 6855–6864.

47 K.-Y. Wang, Z. Yang, J. Zhang, S. Banerjee, E. A. Joseph, Y.-C. Hsu, S. Yuan, L. Feng and H.-C. Zhou, Creating hierarchical pores in metal–organic frameworks via postsynthetic reactions, *Nat. Protoc.*, 2022, DOI: [10.1038/s41596-41022-00759-41597](https://doi.org/10.1038/s41596-41022-00759-41597).

48 W. Lin, H. Chen, G. Lin, S. Yao, Z. Zhang, J. Qi, M. Jing, W. Song, J. Li, X. Liu, J. Fu and S. Dai, Creating frustrated Lewis pairs in defective boron carbon nitride for electrocatalytic nitrogen reduction to ammonia, *Angew. Chem., Int. Ed.*, 2022, **61**, e202207807.

49 Y. Kong, Y. Li, X. Sang, B. Yang, Z. Li, S. Zheng, Q. Zhang, S. Yao, X. Yang, L. Lei, S. Zhou, G. Wu and Y. Hou, Atomically dispersed Zinc(I) active sites to accelerate nitrogen reduction kinetics for ammonia electrosynthesis, *Adv. Mater.*, 2022, **34**, 2103548.

50 Y. Wang, W. Zhou, R. Jia, Y. Yu and B. Zhang, Unveiling the Activity Origin of a Copper-based Electrocatalyst for Selective Nitrate Reduction to Ammonia, *Angew. Chem., Int. Ed.*, 2020, **59**, 5350.

51 Y. Ma, J. Yu, M. Sun, B. Chen, X. Zhou, C. Ye, Z. Guan, W. Guo, G. Wang, S. Lu, D. Xia, Y. Wang, Z. He, L. Zheng, Q. Yun, L. Wang, J. Zhou, P. Lu, J. Yin, Y. Zhao, Z. Luo, L. Zhai, L. Liao, Z. Zhu, R. Ye, Y. Chen, Y. Lu, S. Xi, B. Huang, C.-S. Lee and Z. Fan, Confined growth of silver-copper Janus nanostructures with {100} facets for highly selective tandem electrocatalytic carbon dioxide reduction, *Adv. Mater.*, 2022, **34**, 2110607.

52 D. Chen, L.-H. Zhang, J. Du, H. Wang, J. Guo, J. Zhan, F. Li and F. Yu, A tandem strategy for enhancing electrochemical CO<sub>2</sub> reduction activity of single-atom Cu-S<sub>1</sub>N<sub>3</sub> catalysts via integration with Cu nanoclusters, *Angew. Chem., Int. Ed.*, 2021, **60**, 24022–24027.

53 L. Lin, T. Liu, J. Xiao, H. Li, P. Wei, D. Gao, B. Nan, R. Si, G. Wang and X. Bao, Enhancing CO<sub>2</sub> Electroreduction to Methane with a Cobalt Phthalocyanine and Zinc–Nitrogen–Carbon Tandem Catalyst, *Angew. Chem. Int. Ed.*, 2020, **50**, 22408–22413.

54 T. Zhang, J. C. Bui, Z. Li, A. T. Bell, A. Z. Weber and J. Wu, Highly selective and productive reduction of carbon dioxide to multicarbon products via in situ CO management using segmented tandem electrodes, *Nat. Catal.*, 2022, **5**, 202–211.

55 W. He, J. Zhang, S. Dieckhöfer, S. Varhade, A. C. Brix, A. Lielpetere, S. Seisel, J. R. C. Junqueira and W. Schuhmann, Splicing the active phases of copper/cobalt-based catalysts achieves high-rate tandem electroreduction of nitrate to ammonia, *Nat. Commun.*, 2022, **13**, 1129.

56 C. Chen, X. Yan, Y. Wu, S. Liu, X. Zhang, X. Sun, Q. Zhu, H. Wu and B. Han, Boosting the productivity of electrochemical CO<sub>2</sub> reduction to multi-carbon products by enhancing CO<sub>2</sub> diffusion through a porous organic cage, *Angew. Chem., Int. Ed.*, 2022, **61**, e202202607.

57 H. K. Lee, C. S. L. Koh, Y. H. Lee, C. Liu, I. Y. Phang, X. Han, C.-K. Tsung and X. Y. Ling, Favoring the unfavored: Selective electrochemical nitrogen fixation using a reticular chemistry approach, *Sci. Adv.*, 2018, **4**, eaar3208.

58 W.-J. Sun, H.-Q. Ji, L.-X. Li, H.-Y. Zhang, Z.-K. Wang, J.-H. He and J.-M. Lu, Built-in electric field triggered interfacial accumulation effect for efficient nitrate removal at ultra-low concentration and electroreduction to ammonia, *Angew. Chem., Int. Ed.*, 2021, **60**, 22933–22939.

59 W. Qiu, X. Chen, Y. Liu, D. Xiao, P. Wang, R. Li, K. Liu, Z. Jin and P. Li, Confining intermediates within a catalytic nanoreactor facilitates nitrate-to-ammonia electrosynthesis, *Appl. Catal., B*, 2022, **315**, 121548.

60 D. Yang, Q. Zhu and B. Han, Electroreduction of CO<sub>2</sub> in ionic liquid-based electrolytes, *The Innovation*, 2020, **1**, 100016.

61 Y. Zhong, H. Xiong, J. Low, R. Long and Y. Xiong, Recent progress in electrochemical C–N coupling reactions, *eScience*, 2022, DOI: [10.1016/j.esci.2022.1011.1002](https://doi.org/10.1016/j.esci.2022.1011.1002).

62 R. Wang, S. Jia, L. Wu, X. Sun and B. Han, CO<sub>2</sub>-involved electrochemical C–N coupling into value-added chemicals, *Chem. J. Chin. Univ.*, 2022, **43**, 20220395.

63 S. Wang, T. Feng, Y. Wang and Y. Qiu, Recent Advances in Electrocarboxylation with CO<sub>2</sub>, *Chem. – Asian J.*, 2022, **17**, e202200543.

64 Y. Wang, Z. Zhao, D. Pan, S. Wang, K. Jia, D. Ma, G. Yang, X.-S. Xue and Y. Qiu, Metal-free electrochemical carboxylation of organic halides in the presence of catalytic amounts of an organomediator, *Angew. Chem., Int. Ed.*, 2022, **61**, e202210201.

65 X. Sun, Q. Zhu, J. Hu, X. Kang, J. Ma, H. Liu and B. Han, N, N-Dimethylation of nitrobenzenes with CO<sub>2</sub> and water by electrocatalysis, *Chem. Sci.*, 2017, **8**, 5669–5674.

66 Z.-H. Lyu, J. Fu, T. Tang, J. Zhang and J.-S. Hu, Design of ammonia oxidation electrocatalysts for efficient direct ammonia fuel cells, *EnergyChem*, 2022, DOI: [10.1016/j.enchem.2022.100093](https://doi.org/10.1016/j.enchem.2022.100093).

67 D. Li, N. Xu, Y. Zhao, C. Zhou, L.-P. Zhang, L.-Z. Wu and T. Zhang, A Reliable and Precise Protocol for Urea Quantification in Photo/Electrocatalysis, *Small Methods*, 2022, **6**, 2200561.

68 Y. Huang, Y. Wang, Y. Wu, Y. Yu and B. Zhang, Electrocatalytic construction of the C–N bond from the derivates of CO<sub>2</sub> and N<sub>2</sub>, *Sci. China: Chem.*, 2022, **65**, 204–206.

69 X. Song, L. Xu, X. Sun and B. Han, In situ/operando characterization techniques for electrochemical CO<sub>2</sub> reduction, *Sci. China: Chem.*, 2022, DOI: [10.1007/s11426-021-1463-6](https://doi.org/10.1007/s11426-021-1463-6).

70 Y. Zou and S. Wang, An Investigation of Active Sites for electrochemical CO<sub>2</sub> Reduction Reactions: From In Situ Characterization to Rational Design, *Adv. Sci.*, 2021, **8**, 2003579.

